

Multispectral-TIR Data Analysis by Split Window Algorithm for Coal Fire Detection and Monitoring

Bushra Praveen¹, Deepmala Gupta²

^{1,2}Geosciences and Geohazards Department, IIRS ISRO, Dehradun, India

Abstract: Coal fires are common and serious phenomena in most coal producing countries in the world. Coal fires not only burn valuable non-renewable coal reserves and severely affect the environment, but also sometimes cause loss of life and property. Thus, it is very important to monitor coal fire. Remote sensing provides a useful technique for investigating environmental degradation in general and detecting and monitoring of coal fires in particular. Jharia coal field is an exclusive store house of prime coking coal in the country. In this study, an attempt has been made to retrieve land surface temperature (LST) over Jharia coal field from ASTER multi-spectral TIR data sets acquired in 2006 and 2009 by split window algorithm. Land surface temperature (LST) is an important geophysical parameter used for precisely detecting thermal anomalous pixels. The water vapor content of the atmosphere and atmospheric transmittance in TIR region was determined from MODIS data. Thermal emissivity of the land surface was determined by a hybrid technique adopting NDVI based model and knowledge based approach. LST was determined by split window algorithm using ASTER TIR channels 13 and 14 where atmospheric transmittance and thermal emissivity of the land surface were used as essential inputs. Finally, histogram based separation of thermally anomalous pixels facilitates for detection and monitoring of coal fire affected areas. It is observed that the coal fire affected area has been increased substantially during the observation period (2006-2009).

Keywords: Coal fire, Remote Sensing and GIS, Emissivity.

I. Introduction

Coal is formed from organic matter with high carbon content, which when exposed to certain conditions (temperature, moisture, oxygen etc.) tends to ignite spontaneously at rather low temperatures. Thousands of coal fires are burning around the world including China, India and Indonesia. Australia also experiences similar problems on a smaller scale. The threat fire presents depends on aspects such as the nature and amount of flammable material, the ventilation system arrangement, the duration of the fire and the extent of the spread of combustion product. The problem of mine fire is as old as the history of the mine which propagates in a creeping fashion along mine shafts and cracks in geologic structures. Due to fires in underground as well as surface mines, not only a considerable amount of resources is lost, but the entire mine environment is badly affected. Those burning underground can be difficult to locate and many cannot be extinguished. Fires can cause the ground above to subside, their combustion gases are dangerous to life, and breaking out to the surface can initiate surface wildfires. Coal seams can be set on fire by spontaneous combustion or contact with a mine fire or surface fire. Mining of coal is carried out for centuries because of its various aids such as source of fuel, electricity etc. Unscientific mining and extraction of Coal causes several hazards such as land subsidence and surface and subsurface coal fire. Open cracks and fissures in the land surface serves as inlets for oxygen (Prakash, Fielding, Gens, Van Genderen, & Evans, 2001). As the burned coal turns into ash, often the rock overburden can no longer be supported and deep cracks open up. Eventually, the overburden collapses causing huge damage to surface, buildings, transport network, etc. (Gangopadhyay, Maathuis, & Van Dijk, 2005).

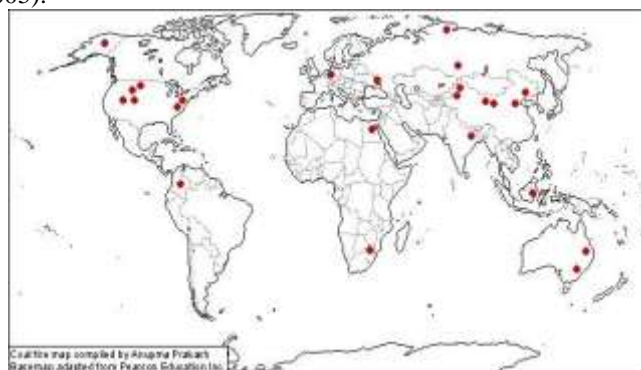


Figure 1 coal fire map of world

I. Need of the study

Coal fires generally increase the temperature of the surrounding areas (Prakash, Gupta, & Saraf, 1997). Urban and human settlements (buildings, road and railway networks etc.) in and around Jharia are facing the threat of subsidence. Subsidence issues have not only affected the surface properties but also caused financial and social problems in the society. Burning of fires beneath the ground and subsidence phenomena related to it pose serious challenge to the scientific community. The results of this study would help to better assess and monitor the coal fire. Here, some important harmful effect of coal fire is

- It has been noted that greenhouse gas emissions from coal fires are significant enough to create a global impact.
- Apart from consuming a valuable resource, it poses enormous operational difficulties by increasing the cost of production or by making existing operations uneconomical.
- Noxious gases such as Sox, NOx and CO often affect the immediate surroundings of an active coal fire.
- Millions of people are affected from several lungs and skin diseases due to these poisonous gases from coal fire.
- Widespread cracking as the burned coal turns into ash, voids are created and often the rock overburden can no longer be supported and deep cracks open up. Eventually the surface collapses, which can cause extensive damage to agricultural land, buildings and transport networks

2.1. Problem statement and Motivation

Coal as a fossil fuel can catch fire by both natural and man-made causes. Some causes of coal fires can be found in:

- Spontaneous combustion
- External heat sources (e.g. illegal distillation of alcohol in Indian coal mines) □ Human induced (careless acts of mine workers).

Spontaneous combustion is one of the most frequent reasons for coal fires. The term 'spontaneous combustion' means that coal can start to burn without any recognizable outer influence. It is caused by coals ability to react with oxygen contained in the air. As a result of the oxidation process the temperature of the coal starts to rise. If the temperature reaches a certain temperature noxious gases are produced such as carbon dioxide. Finally, if the temperature still continues to rise the coal reaches the flash point and starts to burn.

Spontaneous combustion depends, amongst others:

- on coal type,
- temperature,
- availability of oxygen,
- exposure to surface,
- thickness of coal seam,
- As well as methods of mining.

Regarding Jharkhand research says that no single reason can be attributed to the fire. Jharkhand coal is not very prone to auto-oxidation. It is not only the Jharia or its adjoining areas which are affected but areas like north Karanpura coalfield, East Parej coalfield are also under the grip of coal mine fire.

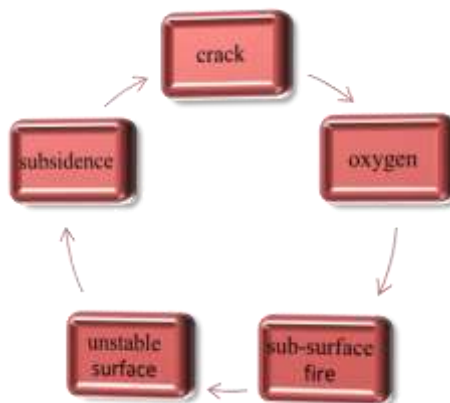


Figure 2 Relationship between subsurface coal fire and subsidence Motivation

The application of remote sensing in monitoring the environmental impacts of human activity is immense. Several environmental hazards like coal-fire, Subsidence due to mining activity are being monitored from satellite data .Surface and underground coal fires.

- Jharia coal field (JCF) in India is known for its high grade coal and its association with coal fire.
- Coal fire destroys valuable coal resources and is the main reason of land subsidence and affecting regional environment.
- Advance technique of ASTER data which has 5 TIR bands with ground resolution of 90 m is big enough to penetrate cracks of active fire.
- It can detect very small differences in radiance as it has 12 bit signal quantization level.

Aim and objectives

The main focus of this research is spatial and temporal dynamics of coal fire during 2006 and 2009 by thermal emissivity and thermal anomaly detection.

- Derivation of LST map from ASTER night time data of JCF using split window algorithm.
- Relative thermal anomaly monitoring and mapping from radiant temperature image.

Research Questions

- Whether split window algorithm is useful in deriving LST.
- Land surface temperature and coal fire affected area has whether increased or decreased during 2006 and 2009. □How LST is useful in case study.
- What are the factors are important for LST and thermal anomaly.

Theory and Literature Review

Thermal Remote Sensing

Thermal remote sensing is the branch of remote sensing that deals with the acquisition, processing and interpretation of data acquired primarily in the thermal infrared (TIR) region of the electromagnetic (EM) spectrum. In thermal remote sensing we measure the radiations 'emitted' from the surface of the target, as opposed to optical remote sensing where we measure the radiations 'reflected' by the target under consideration (Kahle (1980), Sabin's (1996) and Gupta (1991).

In case of high temperature object conditions, such as forest or mine fire, remote sensing can give a good synoptic view of the area under consideration. In the entire electromagnetic spectrum, 3–60 mm is considered as thermal infrared, whereas 3–5 and 8–12 mm is actually used in thermal remote sensing. It is a well-known fact that all natural targets reflect as well as emit radiations. In the TIR region of the EM spectrum, the radiations emitted by the earth due to its thermal state are far more intense than the solar reflected radiations and therefore, sensors operating in this wavelength region primarily detect thermal radiative properties of the ground material. However, as also discussed later in this article, very high temperature bodies also emit substantial radiations at shorter wavelengths. As thermal remote sensing deals with the measurement of emitted radiations, for high temperature phenomenon, the realm of thermal remote sensing broadens to encompass not only the TIR but also the short wave infrared (SWIR), near infrared (NIR) and in extreme cases even the visible region of the EM spectrum.

In thermal remote sensing, radiations emitted by ground objects are measured for temperature estimation. These measurements give the radiant temperature of a body which depends on two factors - kinetic temperature and emissivity.

Spectral Emissivity

Emissivity is a measure of an object's ability to emit infrared energy. Emitted energy indicates the temperature of the object .it is an important measurement in energy balance applications and can be especially when determined by TIR. TIR surface is highly dependent on thermal emissivity of surface defined as the ratio of the emitted radiation at a given temperature to the black body radiation at the same temperature. Emissivity denoted by epsilon (ϵ) is a ratio and varies between 0 and 1. For most natural materials, it ranges between 0.7 and 0.95. Emissivity depends on two main factors: composition and surface geometry. Dark materials absorb more and therefore emit more energy than light materials. Silica is an important constituent in earth's crust, is inversely related to emissivity (in the 8-14 μ m region) therefore presence of silica, which has low emissivity, significantly affects the bulk emissivity of an assemblage. Moreover, smooth surface have lower emissivity than rough surfaces (Gupta r.p, 2003, pg. 190)

The emissivity of natural surfaces may vary significantly due to differences in soil structure, soil composition, organic matter, moisture content and also differences in vegetation cover characteristics. Hence the physical surface temperature is important as it is one of the key factors in determining the exchange of energy and matter between the Earth's surface and the atmosphere. It is therefore an important measurement in energy-

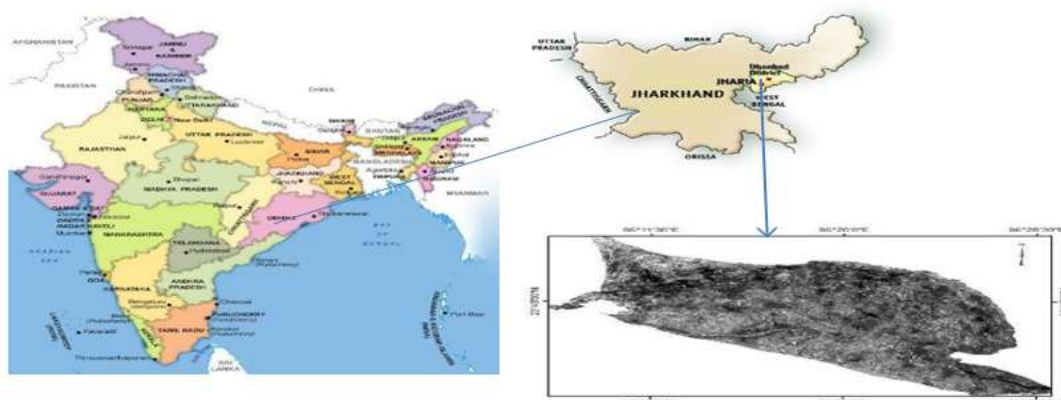
balance applications, and can be especially useful when determined by thermal-infrared (TIR) remote sensing (van de Griend, Prince 1980 et al).

As emissivity decides the amount of energy that will be released from a hot body it makes a significant contribution to the radiant temperature of a surface. Most of the earth's surface falls within the emissivity range of 0.85-0.99. (Rees.1990).

Study Area and Materials / Data Used

Jharia coal field (JCF) is a treasure trove of the best quality prime coking coal of the country. It is situated near Dhanbad town lying at 260 km in North-West of Kolkata and at 1150 km in the South-East of Delhi.

This region is situated between latitude 23° 35' N to 23° 55' and longitude 86°05' E to 86° 30' E. The coal field is spread over an area of 450 sq. km approximately.



This region is situated between latitude 23° 35' N to 23° 55' and longitude 86°05' E to 86° 30' E. The coal field is spread over an area of 450 sq. km approximately.

Mining History of Jharia Coal Field

JCF is the largest coal producer in India with 23 big underground and 9 open cast mines. The mining activities in these coal fields started in 1894. Bharat Coking Coal Limited (BCCL) operates on the majority of area which is about 258 sq. km. (57 percent of the coalfield) with Tata Iron and Steel Co. (TISCO) and the Indian Iron and Steel Co. (IISCO) holding another 32 sq. km., and the remaining areas are mostly occupied by industrial, forest, and Agricultural areas (Prasad 1989; Bharat 1991; Sinha 1989). The history of coalmine fire in Jharia coalfield can be traced back to 1916 when the first fire was detected. More than 70 mine fires are reported from this region.

According to the investigation made after Nationalization, 70 fires were known to exist in BCCL covering an area of 17.32 SQ KM. It was estimated that about 37 million tons of good quality prime coking coal was destroyed and about 1864 million tons coal has been blocked due to these fires. Subsequently 7 more fires were also identified. These 77 fires were spread over in 41 collieries of BCCL.

Geology

The coal field belongs to Gondwana group of Permian age and has Talchir, Barakar, and Barren and Raniganj measures. It is sickle shaped coal field occurring in the form of a basin truncated with a major boundary fault on the southern flank. The coal field is surrounded by metamorphic rocks made of granite, quartzite's, mica schist's and amphibolies. Gneisses are dominant rock type.

The basement metamorphic rocks are overlain by the Talchir formation followed by the Barakar formation which is the main coal-bearing horizon. Above it comes the Barren measure followed by the Raniganj formation which is also coal bearing.

The various coalfields are separated from each other by Precambrian crystalline outcrops. Geological considerations, however, suggest that various basins were once connected with each other through sedimentary strata and lie scattered today as a result of erosion of the overlying strata (Verma et. al., 1973). This elliptical shaped basin is surrounded on all sides by horsts of Precambrian gneisses (Ghosh 1999).

Structurally it is a large elongated structural basin which includes a number of small open and elongate domes and basins trending east-west parallel to that of the major basin (Ghosh and Mukhopadhyay, 1985).

II. Structural lineament

Lineament is an important geological feature. In fire affected coal fields like Jharia coalfield the, nature of lineament-fault pattern is of particularly important to understand possible nature of fire propagation. The basin slopes very gently (5-10°) towards south near the

Southern boundary, the slope of the basin becomes steeper and then the direction reverses towards north (slope amount (20°-30°). The broad structure within the basin is that of a large scale elongated doubly plunging open syncline (Chandra & Chakraborty 1989). There are number of smaller domes and basins within the larger structure. These are very open and somewhat elongated and trends E-W parallel to the trend of the major basin. On either side of the oval outcrops of the sediments, long, narrow horsts of pre-cambriangiess are exposed with the basin itself. The most important are Dugdha high and Durma inlier in the north-east and the Pathardih high in the east.

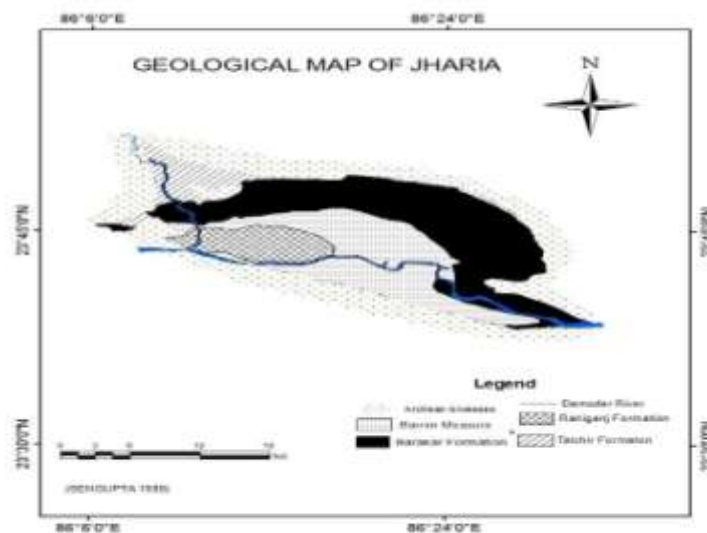


Figure 3 Geological map of Jharia coal field

The Damodar Valley coalfield is regarded as an 'outlier' in the Archaean basement area. The southern boundary of the basin is demarcated by a great boundary fault. Besides the Boundary Fault, the coalfield is traversed by a number of other major and minor faults. Ghosh and Mukhopadhyay (1985) concludes that unequal displacement along the longitudinal and transverse faults results in dome and basins in the coalfield. The

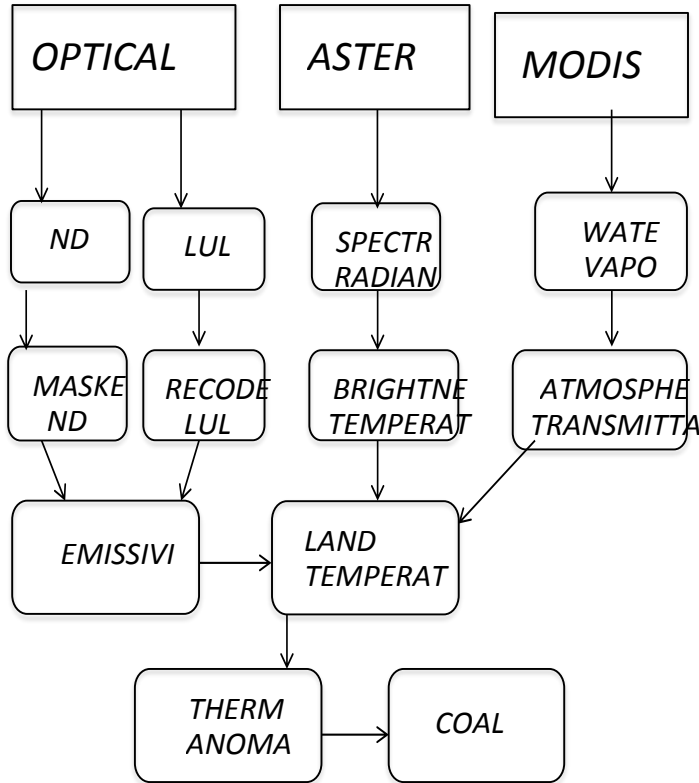
Archaean-Gondwana boundary forms a semicircular arch towards the north-eastern part of the basin and penetrates to a certain extent within the basin itself. Some of the important inliers of the Archaean depositions in this field are Dugdha-high and Damra-inlier in the north-west and Patherdih-high in the east (Ghosh, 1999). Two types of igneous intrusive are met within the Jharia Coalfield; the mica peridotite and the dolerite. The mica peridotite occurs as dykes and sills all over the coalfield and has devolatilized the coal reserves extensively forming what is known as Jhama or natural coke. The resources of Jhama are estimated to be over 1200 million tones. The dolerite with limited effect on coal occurs as dykes which are confined mainly to the western part of the coalfield (CIL, 1993).

Data used

Type	Date / Year	Resolution	Purpose
ASTER night time data	2006 and 2009	90 m	Calculation of radiance and brightness temperature
LISS 3	2006	22 m	Calculation of NDVI and emissivity
LANDSAT	2009	30 m	Calculation of NDVI and emissivity
MODIS Data	2006-2009	1000 m	Calculation of water vapor and transmittance

- ASTER night time 25 oct.2006 & 27 Nov 2009.
- LISS 3 25 oct.2006 and LANDSAT 7 ETM 27 Nov 2009 optical data. □MODIS data

**Remote Sensing Satellite data
Methodology**



Overall methodology Flow Diagram

Retrieval of Spectral Radiance from DN image of satellite.

The relationship between spectral radiance and digital numbers of raw satellite data is called calibration (Chatterjee et.al, 2006). Chandaret.alhas been presented Equation and parameters to convert calibrated digital number (Q_{cal}) from multiple sensors to at-sensor spectral radiance (L_{λ}). Here, post calibration parameter cut off spectral radiance ($L_{min\lambda}$ and $L_{max\lambda}$) for minimum (1) and maximum (255) quantized calibrated digital number of 8 bit.

$$L_{\lambda} = \left(\frac{L_{max\lambda} - L_{min\lambda}}{Q_{calmax} - Q_{calmin}} \right) (Q_{cal} - Q_{calmin}) + L_{min\lambda}$$

Where

- L_{λ} spectral radiance at the sensor's aperture [$W / (m^2 sr \mu m)$]
- Q_{cal} Quantized calibrated pixel value [DN]
- Q_{calmin} Minimum quantized calibrated pixel value corresponding to $L_{min\lambda}$
- Q_{calmax} Maximum quantized calibrated pixel value corresponding to $L_{max\lambda}$
- $L_{min\lambda}$ spectral at-sensor radiance that is scaled to Q_{calmin} [$W / (m^2 sr \mu m)$]
- $L_{max\lambda}$ spectral at-sensor radiance that is scaled to Q_{calmax} [$W / (m^2 sr \mu m)$]

Convert the spectral radiance into at-sensor brightness temperature:

The spectral radiance of Landsat thermal data (TM, ETM and TIRS) can be converted to at-sensor brightness temperature. The at-sensor brightness temperature assumes that the Earth's surface is a black body (i.e., spectral emissivity is 1), and includes atmospheric effects (absorption and emissions along path) (Chander et.al, 2009). To convert at-sensor radiance to at-sensor brightness temperature uses prelaunch calibration constants mathematical formula is:

$$T = \frac{K_2}{\ln\left(\frac{K_1}{L_{\lambda}} + 1\right)}$$

L_{λ}

Where;

- T Radiant temperature [K]
- K_2 Calibration constant 2[K]
- K_1 Calibration constant 1[K]

Estimation of NDVI and Emissivity

The Normalized difference vegetation index (NDVI) of different surface covers is used by the Van De Griend and Owe (1993) in logarithmic relationship between NDVI and emissivity for a monotonous savanna environment in Botswana where NDVI is always greater than zero. So this Van De Griend and Owd relationship is only appropriate for similar region used by Griend and Owd. The scaled value of NDVI is used by Casselles et al. (1997) to represent the percentage of vegetation present within pixels and In Gillies et al. (1997), the scaled value of NDVI is termed to as N* as given below:

$$N^* = \frac{NDVI - NDVI_s}{NDVI_v - NDVI_s}$$

Where NDVI_s represents NDVI value of bare soil, and NDVI_v represents NDVI value of full vegetation. Gillies et al. (1997) developed a relationship between N* and fractional vegetation cover or proportion of vegetation, so Fr can be obtained from NDVI i.e.

$$Fr = N^{*2}$$

NDVI is defined as a function of the surface reflectance of visible (red band) and nearinfrared bands (Brunsell and Gillies, 2001): i.e.

$$NDVI = \frac{NIR-RED}{NIR+RED}$$

In this work, pixel integrated NDVI values obtained from optical data of LISS 3 and LANDSAT optical data for computing the thermal emissivity using above relation. Every land-cover has own reflectance in RED and NIR region so that NDVI value changes from one land-cover to other. The area cover by vegetation and soil where NDVI value is greater than and equal to 0.1 Coal, water bodies, rocks, barren land and overburden have higher reflectance in visible region than that in NIR region (Chatterjee et.al, 2006). Hence, NDVI value is negative. For such areas knowledge based emissivity map has been prepared based on spectral absorption properties of surface cover at each pixel value of satellite data (where NDVI values <0.1). Mostly vegetation is not present in such type of area because it is effected by fire and the value of thermal emissivity has been consider 0.92 (Buettner and kern 1965). Finally satellite based thermal emissivity map is generated for different land covers such as vegetation, crop land, barren land, soil cover, river bed, settlement, overburden, opencast quarry and water body. Satellite based thermal emissivity is validated with Field based emissivity. The emissivity can be calculated from NDVI. When NDVI values range from 0.157 to 0.727, Van De Griend and Owe [22] gave an effective equation as follows:

$$\epsilon = 1.0094 - 0.0047 \ln(NDVI)$$

Material	Emissivity Value
Open cast queries	0.99
Overburden	0.93
River bodies	0.99
Soil cover	0.94
Industrial Area	0.92
Vegetation	0.98

Table 7 Emissivity values of different materials

Calculation of atmospheric transmittance:

Atmospheric transmittance is a critical parameter affecting accuracy of LST retrieval using split window algorithm. The thermal radiance is attenuated on its way to the remote sensor. Transmittance depicts the magnitude of the attenuation of the radiance transferring through the atmosphere. It varies with wavelength and viewing angle. Many atmospheric constituents such as water vapour, O3, CO2, and other gases have impacts on the thermal atmospheric transmittance. However, the contents of O3, CO2, and other gases are relatively stable in the atmosphere. Accordingly, their impacts can be assumed as constant and simulated by standard atmospheric profiles. On the contrary, water vapour content is highly variable. Thus the variation of atmospheric transmittance strongly depends on the dynamics of water vapour content in the profile. Consequently, many split window algorithms relate the determination of atmospheric transmittance to the change of water vapour content while assuming other impacts as constant [Sobrino et al. 1991; France and Cracknell 1994; Colletal. 1994]. Here we also follow this general procedure to estimate the essential atmospheric parameter for LST retrieval from ASTER data.

The transmittance gradually decreases with increase of water vapour content in the atmosphere. Therefore, if we know the content of water vapour in the atmosphere, we are able to use the equations to estimate atmospheric transmittance for LST retrieval from ASTER data.

Water vapour content (w)g cm-2	Estimation equations
0.4-2.0	$\tau_{13}=0.979160-0.062918w$ $\tau_{14}=0.968144-0.098942w$

Table 8 Relationship between transmittance and water content in the atmosphere

However, the data about water vapour content in the atmosphere is generally not available, and the measurement of the content is also very difficult due to the constraint from both cost and time. Fortunately the ASTER is on the same satellite platform as MODIS (Moderate resolution Imaging Spectro radiometer), which is a multiple-band remote sensing system for both atmosphere detection and earth earth observation Atmospheric water vapour content can be retrieved from MODIS data using the atmospheric water vapour algorithm and bands 2 and 19. The formula can be as follows:

$$w = [\alpha - I(\rho_{19}/\rho_{2})] / \beta$$

Derivation of LST

Derivation of split window algorithm for LST retrieval is based on the thermal radiance of the ground and its transfer from the ground through the atmosphere to the remote sensor [Qin et al. 2001, Sobrino et al. 1994]. Generally speaking, the ground is not a blackbody. Thus ground emissivity has to be considered for computing the thermal radiance emitted by the ground. Atmosphere has important effects on the received radiance at remote sensor level. Considering all these impacts, the general radiance transfer equation for remote sensing of LST can be formulated as follows:

$$Bi(Ti) = \tau_i [\epsilon_i Bi(Ts) + (1 - \epsilon_i) Li_{\downarrow}] + Li_{\uparrow} \tag{1}$$

Where

Ts= LST,

Ti =brightness temperature in band i, τ_i atmospheric transmittance in band i ϵ_i =ground emissivity.

Bi(Ti) = radiance received by the sensor,

Bi(Ts) = ground radiance,

Li \downarrow and Li \uparrow downward and upward atmospheric radiances, respectively.

Using approximation of atmospheric radiances and linearization of Planck’s equation, Qin et al. [2001] developed their split window algorithm with the following general form for NOAA-AVHRR data:

$$Ts = T4 + A(T4 - T5) + B \tag{2}$$

Where the Ts is LST, T4 and T5 are brightness temperatures computed from thermal channels 4 and 5 of NOAA-AVHRR data, and A and B are the algorithm parameters. Alternating the thermal channels of AVHRR into ASTER bands, we gain the following split window algorithm for ASTER data:

$$Ts = T13 + (T13 - T14) + B \tag{3}$$

T13 and T14 are brightness temperatures of ASTER bands 13 and 14.

The parameters A and B are defined as

$$A = D13/E0 \tag{4}$$

$$B = E1L13 - E2L14 \tag{5}$$

The parameters D, E and L are computed as follows:

$$E1 = D14(1 - C13 - D13)/E0 \tag{6}$$

$$E2 = D13(1 - C14 - D14)/E0 \tag{7}$$

$$E0 = D14C13 - D13C14 \tag{8}$$

$$Li = Bi(T) / [\tau_i Bi(T) / \tau_i T] \tag{9}$$

Ci = $\epsilon_i \tau_i$

$$Di = [1 - \epsilon_i] [1 + (1 - \epsilon_i) \tau_i] \tag{10}$$

Where

i= thermal bands (i=13 and 14) of ASTER.

Simulation indicates that the parameter L_i is a temperature dependent. Thus, we can use a linear regression equation to fit into the L_i curve in order to avoid the complicated computation. Since L_i is a temperature dependent, we may continue the simplification of the algorithm replacing equation into, we have

$$B = E_1(a_{13} + b_{13}T_{13}) - E_2(a_{14} + b_{14}T_{14}) \quad (11) \text{ Reorganization (11)}$$

Gives

$$B = E_1b_{13}T_{13} - E_2b_{14}T_{14} + E_1a_{13} - E_2a_{14}. \quad (12)$$

Substituting into (3) and reorganizing the terms, we get a new form of split window algorithm for ASTER data as follows:

$$T_s = A_0 + A_1T_{13} - A_2T_{14}, \quad (13)$$

where the coefficients A_0 , A_1 , and A_2 are defined as

$$A_0 = E_1a_{13} - E_2a_{14}, \quad (14)$$

$$A_1 = 1 + A + E_1b_{13}, \quad (15)$$

$$A_2 = A + E_2b_{14}. \quad (16)$$

The algorithm requires two essential parameters for LST retrieval: atmospheric transmittance τ_i , and ground emissivity ϵ_i .

Atmospheric transmittance in the thermal window is generally estimated from water vapour content in the atmospheric column. This change is from day to day and along the day. The most practical way to calculate the atmospheric transmittance is through simulation with local atmospheric conditions, especially water content. For a small range of water vapour content the relationship between water vapour content and atmospheric content may be approximated as a linear equation even though the whole one is a curve as described by Franco and Sabrino et al. [1991].

III. Results And Discussion

The highest land surface temperature of Jharia coal field is found to be 50.59 °C (2006) and 61.54 °C (2009) which shows that coal fire has increased from 2006 to 2009. From study it shows that the highly affected area is kusunda where the area of coal fire increased from 1.5 sq. km in 2006 to 2.66 sq. km in 2009. The temperature map extracted from ASTER night time data (25 October 2006 & 27 November 2009) shows a good contrast between anomaly and background. The algorithm is able to produce a reasonable LST image spatial variation of surface heat flux in the region.

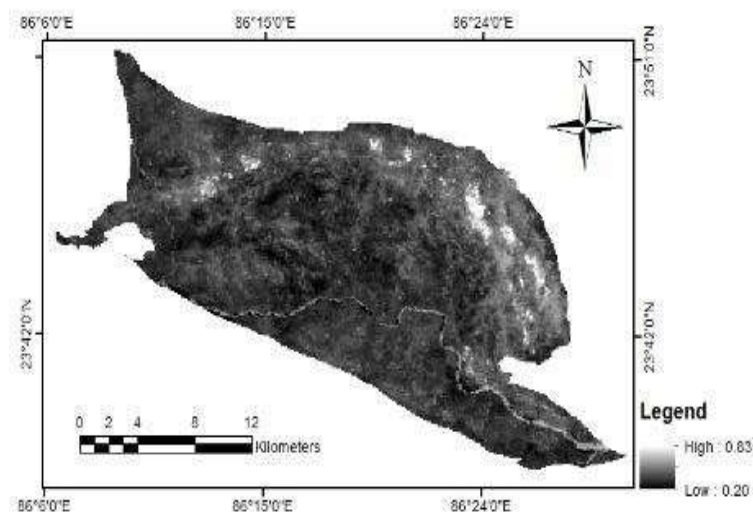
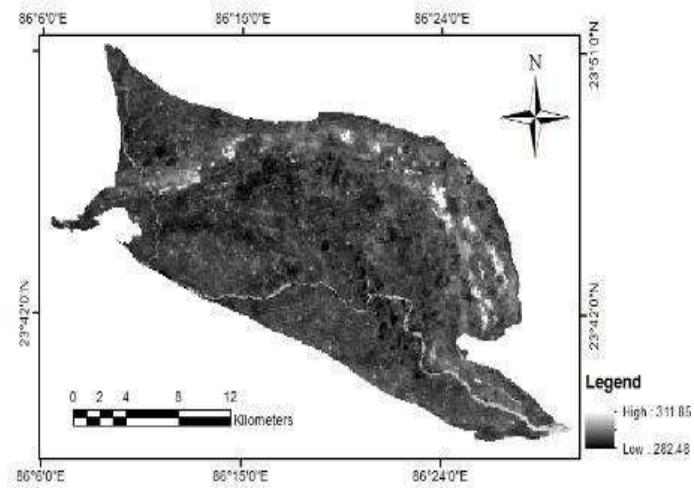


Figure 5 Radiance image of 2006



IV. Figure 6 Radiant Temperature (K) image of 2006.

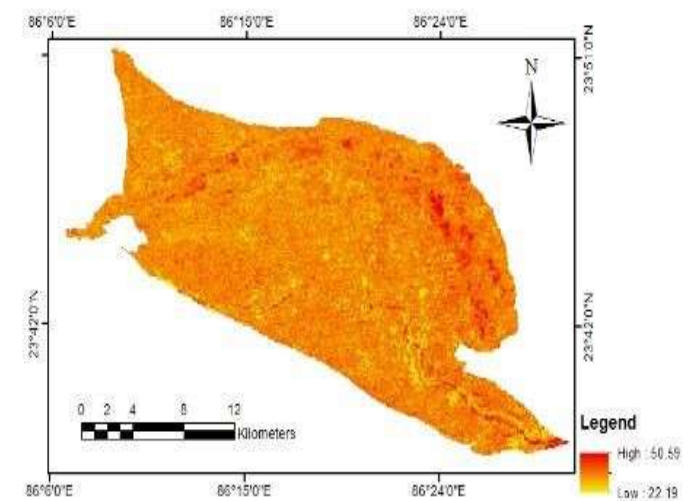
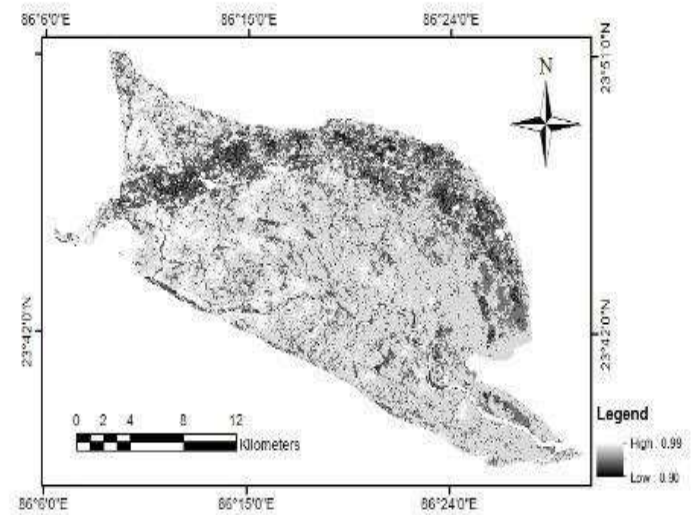


Figure 7.and 8 Land surface temperature image of 2006.

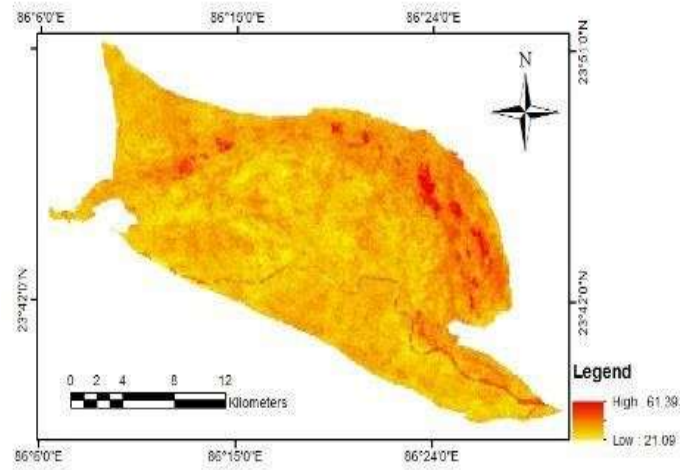


Figure 9 Land surface temperature image of 2009.

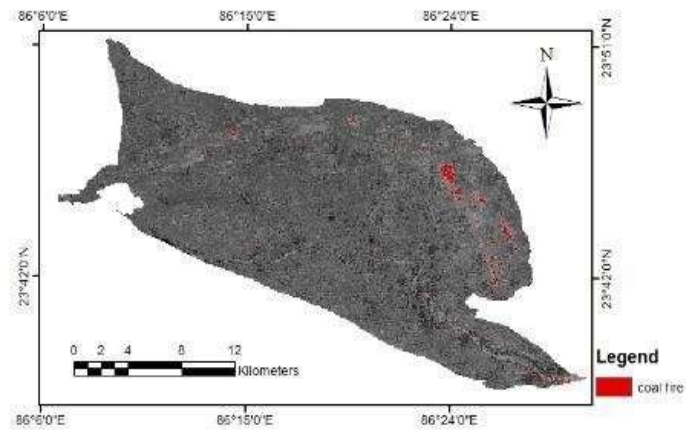


Figure 10 Thermally anomalous pixels delineated by histogram technique from land surface temperature image of 2006.

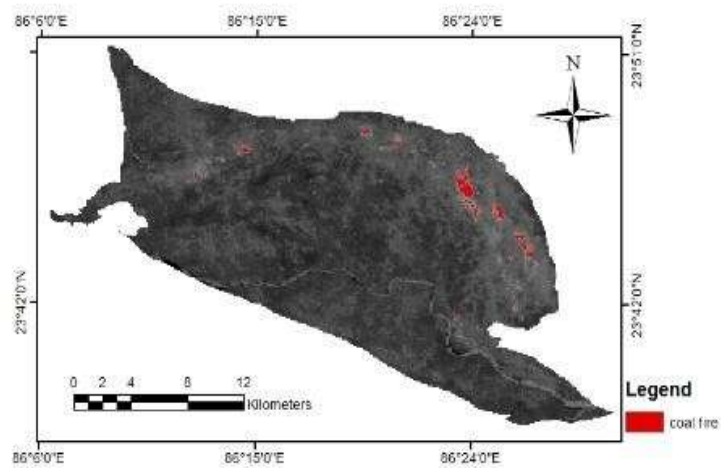


Figure 11 Thermally anomalous pixels delineated by histogram technique from land surface temperature image of 2009.

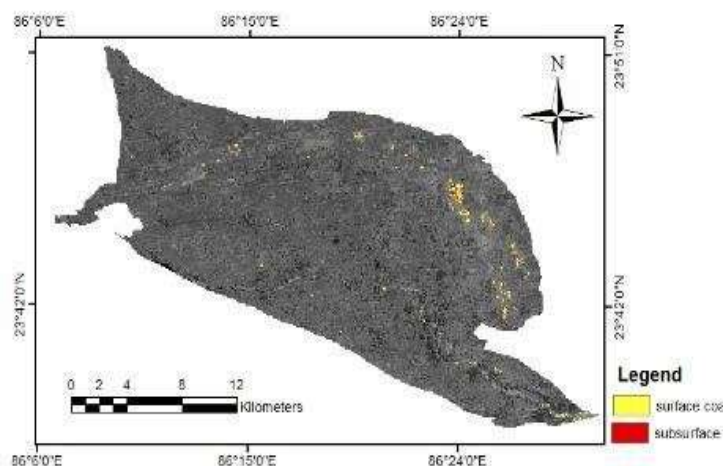


Figure 12 Remote sensing based tentative spatial extent of surface and subsurface coal fire in 2006.

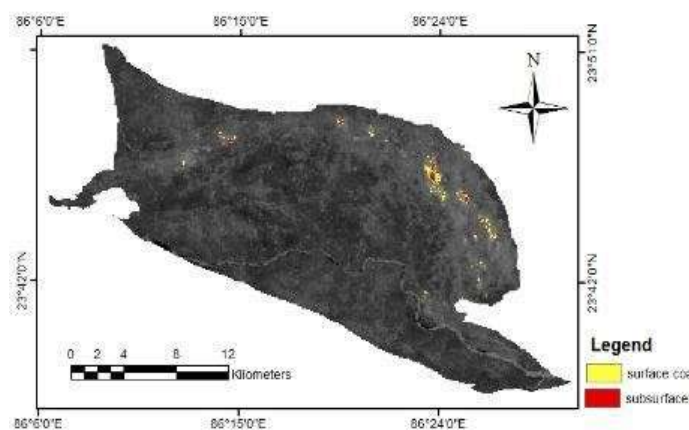


Figure 13 Remote sensing based tentative spatial extent of surface and subsurface coal fire in 2009.

V. Conclusions

Medium resolution thermal remote sensing data such as ASTER night time data are quite useful for coal fire monitoring and mapping. Split window algorithm proposed by Qin et al. [2001] has been adopted for retrieval of land surface temperature from ASTER TIR data. The algorithm requires two essential parameters i.e. atmospheric transmittance and ground emissivity for LST retrieval. In this study, Resource sat LISS III and LANDSAT TM optical data were used to derive NDVI values for the corresponding TIR data. Thermal emissivity image was generated based on NDVI values in vegetation-covered areas and from the knowledge of the spectral absorption properties of surface cover in the remaining areas. ASTER night time data used to calculate spectral radiance using calibration parameters and were converted to radiant temperature using Planck's radiation equation. The result shows that 4.50 sq. km (2006) and 8.05 sq. km (2009) area was thermally anomalous in 2006 and 2009 respectively. Remote sensing based tentative spatial extent of surface and subsurface coal fire are respectively 0.64 sq.km and 0.45 sq.km in 2006 whereas 0.79 sq.km and 0.49 sq. km in 2009. It is observed that the coal fire affected area has been increased during the observation period (2006-2009).

Acknowledgement

This work could not have been possible without the help of many sources-both human and digital countless people have contributed directly or indirectly in the completion of this thesis and I thank you all from the bottom of my heart. My deepest gratitude goes to my respected supervisor Dr. R.S Chatterjee, Scientist "SG", Geosciences and Geo-hazards Dept., Indian Institute of Remote Sensing (IIRS). He was always available as an active support and assistance throughout this project work. I thank him for his useful advice, guidance, patience and encouragement he showed to me. I have learned a lot from him above all the essence of a scientific research and critical comments. I feel indebted to Dr. P.K. Champati ray, Scientist "SG", Head, Geosciences and Geohazards Department for his constant help, cooperation and supervision all through the course.

I would like to express my heartfelt gratitude and thankfulness to Dr. ShovanLalChatteraj Scientist “SD”, Mrs. Richa Sharma Scientist “SD” and Mr. Suresh Kannujiya Scientist “SC”, Indian Institute of Remote Sensing, Course coordinator, Geosciences Department for their constant support and encouragement throughout the course at Geosciences Department, IIRS. I avail this opportunity to express my profound sense of reverence and humble gratitude to Dr. Senthil Kumar, Director, IIRS, and Dr. S.P.S Kushwaha, Dean (Academic), IIRS for their support to stay at beautiful and homely campus of IIRS in Dehradun. My Special thanks to Shailaja Thapa for her support and ideas throughout the project work. I thank all JRF and M.tech senior Bhavana Ghildiyal, Somalin Nath, Gopal Sharma, Vivek Senger, Rohit Kumar. I also thank Ashish Dhiman (Tech-Asst) and Ms. Ramandeep Kaur who has been very active in providing necessary logistics that made my project smoother. I cannot forget my friend Bushra, Shristi, Preety and classmates who have always remained supportive during my course work. Last but not least I would like to express my sincere gratitude to my brothers Sandeep & Sanjay, sisters Neetu, Pinky & Vandana for their continuous support and encouragement and constant love and concern are always over whelming and led me to a great accomplishment.

References

- [1]. Bharat Coking Coal Limited (1991), Mine Fires in the Jharia Coalfield. Bharat Coking Coal Limited, Project and Planning Division, Dhanbad, India, 117 pp.
- [2]. Bharat Coking Coal Limited (2008), Master Plan for dealing with the fire, subsidence and rehabilitation in the leasehold of Bharat Coking Coal Limited, Project and Planning Division, Dhanbad, India.
- [3]. Bhattacharya, A., Reddy, C.S.S., 1992. Airborne scanner survey and data analysis for underground and surface coal mine fire detection in Jharia Coalfield, Bihar. Report from the Geosciences Division Applications Group, National Remote Sensing Agency Hyderabad, (India), Report No.NRSA-AG-GD-TR-2/92.
- [4]. Buettner, K.J.K., Kern, C.D., 1965. The determination of infrared emissivity of terrestrial surfaces. *Journal of Geophysical Research* 70, 1329–1337.
- [5]. Casselles, V., C. Coll, and E. Valor, 1997. Land surface emissivity and temperature determination in the whole HAPEX-Sahel area from AVHRR data. *International Journal of Remote Sensing*, 18:1009-1027.
- [6]. Chandra, D., 1992. Jharia Coalfields, Geological Society of India, Bangalore.
- [7]. Chatterjee, R. S. (2006). Coal fire mapping from satellite thermal IR data – A case example in Jharia Coalfield, Jharkhand, India. *ISPRS Journal of Photogrammetry and Remote Sensing*, 60(2), 113–128. doi:10.1016/j.isprsjprs.2005.12.002.
- [8]. Chatterjee, R. S., Wahiduzzaman, M., Shah, A., Raju, E. V. R., Lakhera, R. C., & Dadhwal, V. K. (2007). Dynamics of coal fire in Jharia Coalfield, Jharkhand, India during the 1990s as observed from space. *CURRENT SCIENCE-BANGALORE-*, 92(1), 61.
- [9]. Ellyett, C. D., & Fleming, A. W. (1974). Thermal infrared imagery of the Burning Mountain coal fire. *Remote Sensing of Environment*, 3(1), 79–86.
- [10]. Floyd F. Sabin, 1997, 3rd ed., remote sensing: Principle and Applications, Waveland press. Gangopadhyay, P. K., Maathuis, B., & Van Dijk, P. (2005). ASTER-derived emissivity and coal-fire related surface temperature anomaly: a case study in Wuda, north China. *International Journal of Remote Sensing*, 26(24), 5555–5571. doi: 10.1080/01431160500291959.
- [11]. Gillies, R.R., and T. Carlson, 1995. Thermal remote sensing of surface soil water content with partial vegetation cover for incorporation into climate models. *Journal of Applied Meteorology*, 34:745-756.
- [12]. Gillies, R.R., T. Carlson, J. Cui, W. Kustas, and K. Humes, 1997. A verification of the 'triangle' method for obtaining surface soil water content and energy fluxes from remote measurements of the normalized difference vegetation index (NDVI) and surface radiant temperature. *International Journal of Remote Sensing*, 18-3145-3166.
- [13]. HongyuanHuo, Xiaoguang Jiang, Xianfeng Song, Zhao-Liang Li, Zhuoyan Ni, and Caixia Gao, 2014. Detection of Coal Fire Dynamics and Propagation Direction from Multi-Temporal Nighttime Landsat SWIR and TIR Data: A Case Study on the Rujigou Coalfield, Northwest (NW) China. *Journal of remote sensing*, (Vol 6, 1234-1259).
- [14]. K. MAO, Z. QIN, J. SHI and P. GONG, 2005. A practical split-window algorithm for retrieving land-surface temperature from MODIS data *International Journal of Remote Sensing* Vol. 26, No. 15, 3181–3204
- [15]. Kuenzer, C., & Dech, S. (2013). Theoretical Background of Thermal Infrared Remote Sensing. In C. Kuenzer & S. Dech (Eds.), *Thermal Infrared Remote Sensing* (Vol. 17, pp. 1–26). Dordrecht: Springer Netherlands.
- [16]. Kuenzer, C., Hecker, C., Zhang, J., Wessling, S., & Wagner, W. (2008). The potential of multi-diurnal MODIS thermal band data for coal fire detection. *International Journal of Remote Sensing*, 29(3), 923–944. Doi: 10.1080/01431160701352147.
- [17]. KAUFMAN, Y.J. and GAO, B.-C., 1992, Remote sensing of water vapor in the near IR from EOS/MODIS. *IEEE Transactions on Geoscience and Remote Sensing*, 30, pp. 871–884.
- [18]. Prakash, A., Gens, R., Vekerdy, Z., 1999. Monitoring coal fires using multi-temporal nighttime thermal images in a coalfield in northwest China. *International Prakash, A., Gupta, R.P., Saraf, A.K., 1997. A Landsat TM based comparative study of surface and subsurface fires in the Jharia Coalfield, India. International Journal of Remote Sensing.*
- [19]. Prasad, R. M. (1989). An Appraisal of Subsidence Problems in the Jharia Coalfield. P. 207229. Proceedings: International Symposium on Land Subsidence, Vol 1. (Dhanbad, India, Dec. 11-15, 1989).
- [20]. Prakash & R. P. Gupta (1998): Land-use mapping and change detection in a coal mining area a case study in the Jharia coalfield, India, *International Journal of Remote Sensing*, 19:3, 391-410
- [21]. Reddy, C.S.S., Srivastav, S.K., Bhattacharya, A., 1993. Application of thematic mapper short wavelength infrared data for the detection and monitoring of high temperature related geo-environmental features. *International Journal of Remote Sensing* 14 (17), 3125–3132. R.P. Gupta, 2003 2nd ed., Remote sensing Geology, Springer.
- [22]. Salisbury, J.W., 1986. Preliminary measurements of leaf spectral reflectance in the 8–14 μm regions. *International Journal of Remote Sensing* 7 (12), 1879–1886.
- [23]. Salisbury, J.W., Milton, N.M., 1988. Thermal infrared (2.5–13.5 μm) directional hemispherical reflectance of leaves. *Photogrammetric Engineering and Remote Sensing* 54 (9), 1301–1304.
- [24]. Singh, G., Jain, M. K., Paul, B., Gupta, R. D., & Raju, E. V. (n.d.). Clusterization of mines for obtaining comprehensive environmental clearance: A case study of BCCL lease hold areas. *Journal of Indian School of Mines, Special Volume 2010*, 13–20. An algorithm to retrieve land surface temperature from ASTER thermal band data for agricultural drought monitoring Zihaoqin et al.